



Hollow silica and silica-boron nano/microparticles for contrast-enhanced ultrasound to detect small tumors

Alexander Liberman^a, H. Paul Martinez^b, Casey N. Ta^c, Christopher V. Barback^d, Robert F. Mattrey^{e,f}, Yuko Kono^e, Sarah L. Blair^{f,g}, William C. Trogler^b, Andrew C. Kummel^b, Zhe Wu^{d,f,*}

^aUniversity of California, San Diego, Materials Science and Engineering Program, 9500 Gilman Drive Mail Code 0418, La Jolla, CA 92093, USA

^bUniversity of California, San Diego, Department of Chemistry and Biochemistry, 9500 Gilman Drive Mail Code 0358, La Jolla, CA 92093, USA

^cUniversity of California, San Diego, Department of Electrical and Computer Engineering, 9500 Gilman Drive Mail Code 0407, La Jolla, CA 92093, USA

^dUniversity of California, San Diego, Department of Radiology, 200 W Arbor Drive, San Diego, CA 92103, USA

^eUniversity of California, San Diego, Department of Radiology, 410 Dickinson Street, San Diego, CA 92103, USA

^fUniversity of California, San Diego, Moores Cancer Center, 3855 Health Sciences Drive, La Jolla, CA 92093, USA

^gUniversity of California, San Diego, Department of Surgery, UCSD, 200 W. Arbor Drive, San Diego, CA 92103, USA

ARTICLE INFO

Article history:

Received 24 February 2012

Accepted 18 March 2012

Available online 11 April 2012

Keywords:

Ultrasound

Nano

Silica

Shells

Imaging

Contrast

ABSTRACT

Diagnosing tumors at an early stage when they are easily curable and may not require systemic chemotherapy remains a challenge to clinicians. In order to improve early cancer detection, gas filled hollow boron-doped silica particles have been developed, which can be used for ultrasound-guided breast conservation therapy. The particles are synthesized using a polystyrene template and subsequently calcinated to create hollow, rigid nanoporous microspheres. The microspheres are filled with perfluoropentane vapor. Studies were performed in phantoms to optimize particle concentration, injection dose, and the ultrasound settings such as pulse frequency and mechanical index. *In vitro* studies have shown that these particles can be continuously imaged by US up to 48 min and their signal lifetime persisted for 5 days. These particles could potentially be given by intravenous injection and, in conjunction with contrast-enhanced ultrasound, be utilized as a screening tool to detect smaller breast cancers before they are detectable by traditional mammography.

© 2012 Elsevier Ltd. All rights reserved.

1. Introduction

Excising non-palpable breast cancers in breast conservation therapy is difficult because surgeons must rely on mammographic localization. Wire localization has been the standard method to localize non-palpable tumors, but the reported positive margin rate from wire-localized excisions of breast cancers is approximately 20–50% [1–3]. This poor performance is partly due to wire movement during patient transport to the operating room as well as manipulation during surgery which results in positive margins with wire localization. Radioactive seeds have also been used for breast conservation therapy with a substantial improvement in performance relative to guide wires [4,5]. Unfortunately, these seeds are rarely used due to short radioactive half-life and the need

to expose both the patient and the operating room personal to radiation. Our proposed method of localizing tumors with nanoparticles detectable with ultrasound (US) has two main advantages: no radiation risk, and it allows for multiple injections to better outline the tumor and its margin for the surgeon to reorient during surgery to ensure complete tumor removal. A recent survey study of breast surgeons practicing in community hospital settings has shown that at least one third are already routinely using intra-operative US [6]. Therefore a new technology that improves US performance could not only replace an older technique that utilizes radioactivity, but could also be readily implemented by clinicians.

Mammographic screening has been shown to decrease mortality rates by 15–25% in several large randomized prospective studies, however, mammographic sensitivity is impaired for non-calcified masses in radiographically dense breast tissue [7]. This data suggests that further improvement in screening accuracy could increase survival. In North America, breast US is most often a targeted examination, limited to the area of concern based on palpation or mammography. MRI has been extremely beneficial for

* Corresponding author. University of California, San Diego, Department of Radiology, 200 W Arbor Drive, San Diego, CA 92103, USA. Tel.: +1 858 246 0759; +1 2623231358 (cell); fax: +1 619 543 6372.

E-mail address: zhewu@ucsd.edu (Z. Wu).

screening high-risk women for breast cancer, evaluating silicone implants, and monitoring response to neoadjuvant chemotherapy. MRI is starting to be employed preoperatively to determine a patient's eligibility for breast conservation therapy. Unfortunately, there has not been a demonstrated benefit to pre-operative MRI for improving outcomes of breast conservation, and pre-operative MRI is an expensive procedure with a relatively high false positive rate leading to more biopsies and increasing rates of mastectomy [8]. At present, whole breast US screening can reliably detect ~10 mm diameter tumors [9]. For lesions that remain equivocal after mammographic and standard US evaluation, it has been postulated that contrast-enhanced US (CEUS) could be the problem-solving method [10–12]. The nano/microparticles may be useful for both diagnosis of ~1 mm diameter breast tumors and intra-operative localization to insure complete resection.

Microbubble based contrast agents are clinically used to enhance the US echo signals. All commercially manufactured US contrast agents have lipid, polymer or protein shells encapsulating either air (Albunex, Levovist, Sonovist) or perfluorocarbon gas (Definity, Optison) [13]. These microbubbles generate significant contrast at relatively low acoustic pressure with the color Doppler, power Doppler, or contrast specific imaging techniques available on commercial US systems [13,14]. US pulses, particularly at microbubble resonance induce microbubble destruction at mechanical indices (MI) below 0.3 – MI is a measure of US energy that is the ratio of peak negative pressure and the square root of the transmit frequency. Microbubble destruction causes a decorrelation between two consecutive US pulse that is visible as color on Doppler imaging that has been termed stimulated acoustic emission (SAE). While microbubble destruction can also be detected with contrast specific imaging methods, these techniques were developed to detect the non-linear behavior of microbubbles when exposed to non-destructive US pressures at very low MI [14]. Because tissues respond linearly to US, these techniques are extremely sensitive to the presence of microbubbles and can detect a single microbubble. The non-linear response of microbubbles is related to their ability to expand and contract when exposed to US, which is controlled by the elasticity of the encapsulating shell. Our silica shell is rigid and would not be expected to respond non-linearly; however, the shell was designed to fracture at a given US pressure to not only create a signal on Doppler imaging by SAE, but the release perfluorocarbon gas that is able to expand and contract will generate non-linear signals until it dissolves. Both linear and non-linear signals can be generated from microbubbles depending on particle properties (shell material, shell thickness, encapsulated gas, particle radius, etc.) and the applied signal (pressure, frequency, waveform, etc.) [15]. Tiemann et al. demonstrated that using SAE of air filled cyanoacrylate microbubbles, a high signal is obtained using Doppler imaging from a stationary bolus of particles which have been cast into gelatin [16]. However, the continuous imaging time is brief and the particles are not entirely uniform in size.

As described in a previous report, our group has developed hollow perfluoropentane filled silica shelled particles with a highly uniform size, which can be made from 0.1 to 2 μm in size that can be used as a US contrast agents detectable by Doppler imaging as well as contrast specific imaging for extended periods of time [17]. The rigid shells of these particles allows for extended storage and *in vivo* survival. These hollow silica and silica-boron nano/microparticles can be used as imaging tools in 2-photon microscopy, fluorescence microscopy as well as US imaging [17,18]. This article reports on the continuous imaging time of these hollow silica microparticles, their persistence *in vitro* and *in vivo*, their dependence on the US frequency used in clinical US, the mechanism of imaging, and a demonstration of the imaging technique of silica and silica-boron particles systemically for US imaging in tumor bearing mice.

2. Materials and methods

Tetramethyl orthosilicate (TMOS), trimethyl borate (TMB), perfluoropentane (PFP), and 0.1% poly-L-lysine (PLL) were purchased from Sigma Aldrich (St. Louis, MO). Polystyrene templates were purchased from Polysciences (Warrington, PA). Phosphate buffered solution (PBS) was purchased from Fisher Scientific (Pittsburgh, PA). Micro and nanoshells were tested on two different commercially available US machines. The machines employed were the Siemens Sequoia 512 equipped with Cadence contrast pulse sequencing (CPS) and the Philips iU22. The transducers used were the Acuson 15L8 and Philips L12-5 that are used for breast US imaging. During imaging of particles, US parameters (filters and gains) were optimized in order to maximize signal from particles while reducing background in all cases as is done clinically.

For testing of locally injected microshells, nanoshells and microbubbles, a rabbit model was employed. Four female New Zealand White Rabbits weighing 5 kg each were housed individually in a UCSD approved animal housing facility. Rabbits were fed a commercial pelleted diet (Harlan Teklad) *ad libitum* and kept at 20 °C with a 12 h light/dark cycle. During scans, animals were anesthetized with isoflurane gas with medical air. All animal care and procedures were approved by the UCSD Institutional Animal Care and Use Committee.

For testing of systemic injection of micro and nanoshells, tumor bearing mice were employed. Five week old female nu/nu mice were purchased from Charles River Labs and housed in a UCSD approved animal housing facility. Animals were fed Harlan Teklad rodent feed and kept at 22 °C with a 12 h light/dark cycle. After an acclimation period of ten days, 10⁶ IGROV-1 cells were injected IP into each mouse and the animals were scanned approximately five weeks later. Mice were anesthetized with isoflurane gas and sacrificed by CO₂ asphyxiation after the experiments.

Particles were synthesized as previously described in the literature [17,18,22]. The uniformity of the particles was checked by scanning electron microscopy as shown in Fig. 1. Particles of all sizes were stored dry until needed. Prior to US experiments, particles were weighed and filled with perfluoropentane gas as previously described in the literature and suspended in ultrapure filtered water [17].

3. Results

Initial experiments were performed in order to establish the optimal imaging parameters for the particles with clinical US equipment. The Philips iU22 US scanner was used for imaging with the L12-5 transducer. A 50 μl bolus of 2 μm diameter particles at a concentration of 2 mg/ml was injected into chicken breast phantoms. With color Doppler imaging, the minimum detectable

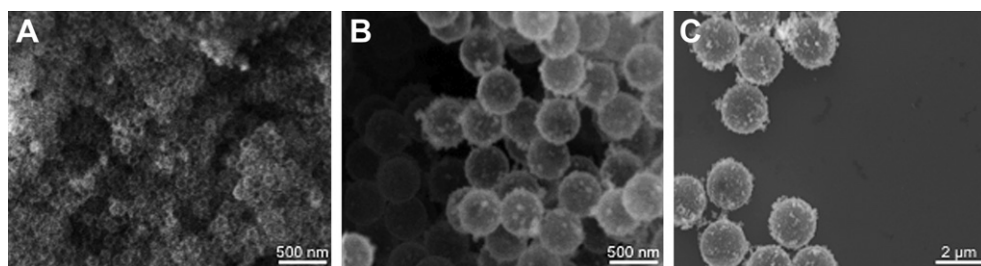


Fig. 1. SEM images of porous hollow silica nano and microshells prepared using a templating sol-gel process. (A) 100 nm diameter nanoshells; (B) 500 nm nanoshells; (C) 2 μm microshells. Note: all have a shell thickness of ~10 nm and a uniform size distribution.

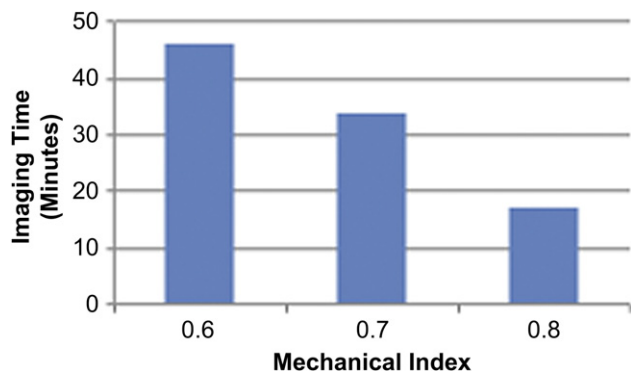


Fig. 2. Continuous imaging time in a chicken breast phantom. A 50 μ l bolus of 2 mg/ml of 2 μ m sized gas filled nanoshells were injected into chicken breast tissue and imaged continuously under color Doppler with different mechanical indices until no usable signal was detectable. The continuous imaging time was greater at low mechanical index.

signal was found at an MI of 0.6, and the maximum allowable MI was 0.8 due to the focus constraints of the transducer. To determine the continuous imaging time, the transducer was fixed using a mechanical arm and the particles were imaged continuously with color Doppler until no signal could be detected. As shown in Fig. 2, the continuous color Doppler imaging time was at least 45 min with low MI of 0.6, but dropped to 18 min at MI 0.8, which was consistent with the expectation that fewer particles were destroyed per US pulse at a low MI.

The *in vitro* imaging lifetime of the particles was investigated by monitoring the color Doppler signal decay over time to assess gas retention within the particles. A 50 μ l solution of 2 mg/ml of 2 μ m particles were injected into the 25 $^{\circ}$ C chicken breasts and imaged for brief periods over the course of 120 h using the color Doppler mode of the Philips iU22; the chicken breasts were kept at 25 $^{\circ}$ C between imaging. The color Doppler data was collected and analyzed for signal area degradation over time. As shown in Fig. 3, a 50 μ l injection containing 100 μ g of particles retained significant signal for five days. This data is consistent with the extremely low diffusion of the perfluoropentane gas within intact particles which has been corroborated in *in vivo* studies.

The optimal US frequency for imaging the particles with a clinical probe was determined using the Siemens Sequoia US machine and 15L8 transducer. 50 μ l of 2 μ m particles were injected in a chicken breast phantom and imaged with color Doppler at a frequency between 7 and 14 MHz. Particles were imaged very briefly while cycling through the frequency range in order to reduce the fraction of particles being extinguished. As shown in Fig. 4, as the frequency was decreased, the signal area produced by

the particles increased significantly. The data was fitted to several functional forms; the correlation with minimal error was an exponential function. Frequencies below 7 MHz were not investigated because the loss of spatial resolution makes these frequencies impractical for breast imaging.

In order to analyze particle behavior as a function of US pressure, CPS imaging was employed. Although Doppler imaging produces a more robust signal, CPS allows us to assess individual events. The 500 nm and 2 μ m gas filled shells were diluted to 0.1 mg/ml and each inserted into a thin wall acoustically transparent chamber and clamped in a water bath. The 15L8 transducer was fixed using a mechanical arm in the water bath perpendicular to the chamber to produce clear images of the sample. As the MI was increased from 0.06 to 1.9 (maximum allowed MI by the FDA), an increasing amount of signal was observed (see Fig. 5A and B). The image brightness in CPS mode corresponds linearly with the number of decorrelation events. In Fig. 5A and B, the fracturing of particles resulted in gold specks which correspond to echo decorrelation events and the resultant signal from the free gas. As the MI was increased, the number of gold specks per area increased dramatically, indicating greater number of particles fractured. As shown in Fig. 5C and D, when the MI was increased stepwise, the signal brightness would reach a local maxima and decay until the MI was again increased. When the reverse experiment was performed (Supplemental Fig. 1) by starting with high MI imaging and progressing to low MI imaging, no peaks were observed in the CPS signal; instead, a monotonic decrease in signal was observed. The data is consistent with the existence of subpopulations of particles each of which have a different MI threshold that fractures its shell.

Four New Zealand White Rabbits were used to study the behavior of the particles *in vivo* over five days. 50 μ l of either 2 mg/ml of 2 μ m and or 2 mg/ml of 500 nm particles were injected into both thighs. 50 μ l of definity microbubbles, a commercially available US contrast agent, were injected at a concentration of 10^8 microbubbles/ml or 10^{10} microbubbles/ml as controls to duplicate the particle concentration of 100 μ g of the 2 μ m and 500 nm particles, respectively. Controls and both shell sizes were imaged using the Siemens Sequoia at an MI of 1.9 and a frequency of 7 MHz for optimal particle detection.

As can be seen from Fig. 6, commercially available microbubbles could only be imaged within a few minutes of the injection on Day 0. Conversely, both the gas filled 2 μ m and 500 nm shells could be detected for four days *in vivo* after the initial injection. Moreover, this *in vivo* data is highly correlated to the previous results shown in an *in vitro* model, consistent with the hypothesis that the perfluoropentane gas does not readily diffuse out of the particles both *in vitro* and *in vivo*. Furthermore, as can be seen from Fig. 6, while the signal diminishes over several days, signal decay is substantially

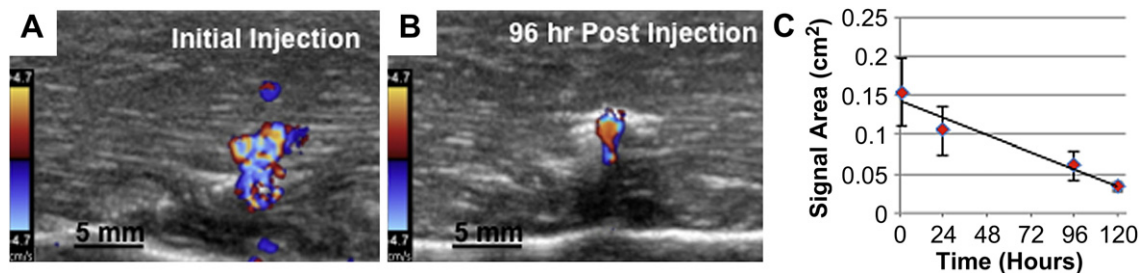


Fig. 3. Persistence in a phantom. (A) Color Doppler image (CDI) of 50 μ l of 2 mg/ml 2 μ m gas filled microshells after injection into a chicken breast phantom kept at 25 $^{\circ}$ C. (B) CDI 96 h after injection. (C) CDI signal area vs. time. As seen here, there was substantial signal present from the same injection up to 120 h after initial injection which was consistent with high gas retention, high *in vitro* stability, and low color Doppler signal decay.

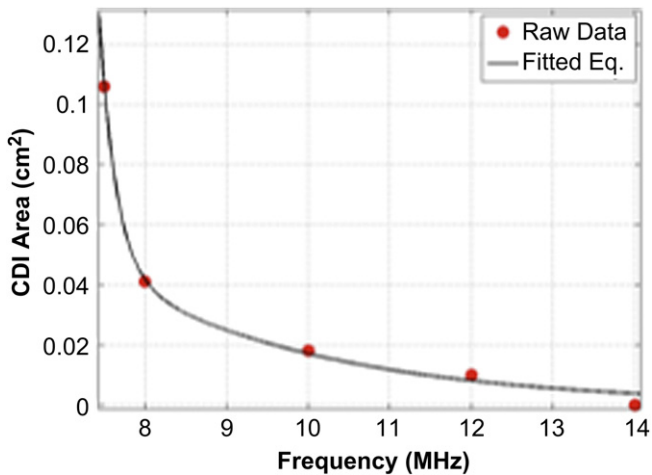


Fig. 4. Area of CDI signal vs. transducer frequency. A 50 μ l bolus of 2 mg/ml 2 μ m of gas filled microspheres were injected into a chicken breast phantom and imaged at multiple frequencies using a 15L8 Sequoia transducer. As frequency decreased, signal area increased exponentially. The red dots are the raw data points and the black line is the fitted equation, $f(x) = 0.74 e^{-0.38x} + 4.13 \times 10^{14} e^{-4.9x}$ $r^2 > 0.99$. (For interpretation of the references to colour in this figure legend, the reader is referred to the web version of this article.)

similar to the *in vitro* data suggesting that blood flow and muscle movement have a minimum effect on particle and/or gas loss. The results shown in Fig. 6 also indicate that the particles do in fact stay stationary once injected into tissue and do not excavate from the injection site despite being in a high strain zone such as thigh muscle tissue.

Two nu/nu mice with intraperitoneal IGROV-1 ovarian tumors were used to study the US behavior of particles when given systemically. Prior to particle delivery, excess fluid from the peritoneal cavity was drained to reduce fluid pressure to reduce the likelihood that the particles could leak out of the needle tract. 200 μ g of PFP filled 2 μ m or 500 nm particles were diluted into 3 ml of saline and injected into the peritoneum. Intraperitoneal injections have been previously been used for systemic delivery in murine models [19–21]. The particles were imaged at high MI using CPS imaging intermittently over 2 h.

The particles were tested for their ability to accumulate within a tumor and be imaged by CEUS. As shown in Fig. 7A, these mice have advanced cancer with an approximately 1 cm tumor mass (red arrow); however, due to the large size of the tumor it is possible to image through the tumor with great confidence. In Fig. 7B–D acquired in the transverse plane, the bottom boundary seen in the image (blue arrow) is actually the bottom of the mouse and the mound like region on the bottom (green arrow) is the spinal column. Visualizing the particles with CPS in an individual frame is extremely difficult because: 1) with high MI CPS imaging, background tissue signal is not completely suppressed; and 2) the signal from each particle event persists for a few frames and is dynamic. Image processing techniques were used to generate Fig. 7D which (a) corrects motion due to movement of the transducer and the breathing of the mouse, (b) selects the signal from single particles by applying a high-pass filter, (c) integrates the particle signal from the entire series of frames acquired over the same location, and (d) displays the signal from the particles as a red-yellow heat map superimposed on the gray scale B-Mode image. As can be seen from Fig. 7D, signal generated by the particles could be seen specifically in the tumor 1 h after injection.

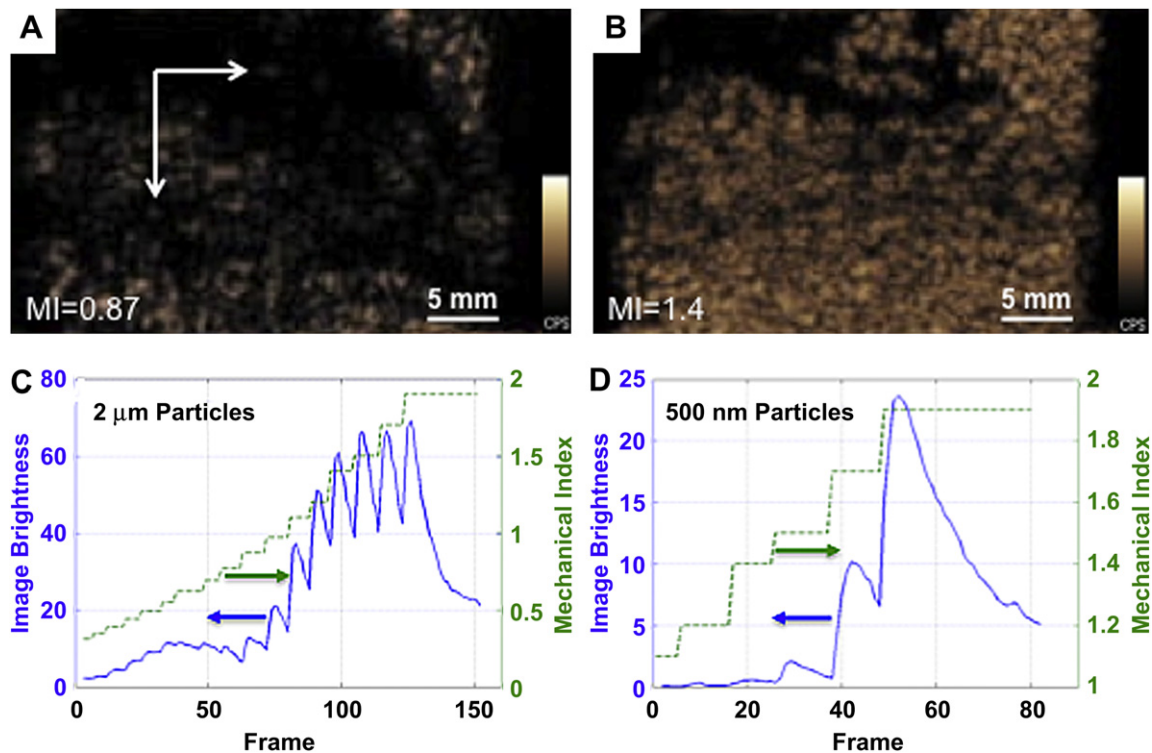


Fig. 5. Effect of ascending mechanical index (MI) on CPS imaging of gas filled silica nano and Microspheres. Particles were imaged using CPS mode with MI scaling from 0.06 to 1.9. (A) CPS image of 100 μ g/ml of gas filled 2 μ m microparticles at MI = 0.87. Each gold speck is a single event (white arrows). (B) CPS image 100 μ g/ml of gas filled 2 μ m microparticles at MI = 1.4. The large density of gold specks corresponds to a large number of particles being imaged. (C) Signal brightness plotted against MI for 2 μ m gas filled microspheres. (D) Signal brightness vs. MI for gas filled 500 nm silica nanoshells. Note that the 500 nm particles generated less signal than the 2 μ m particles at the same MI.

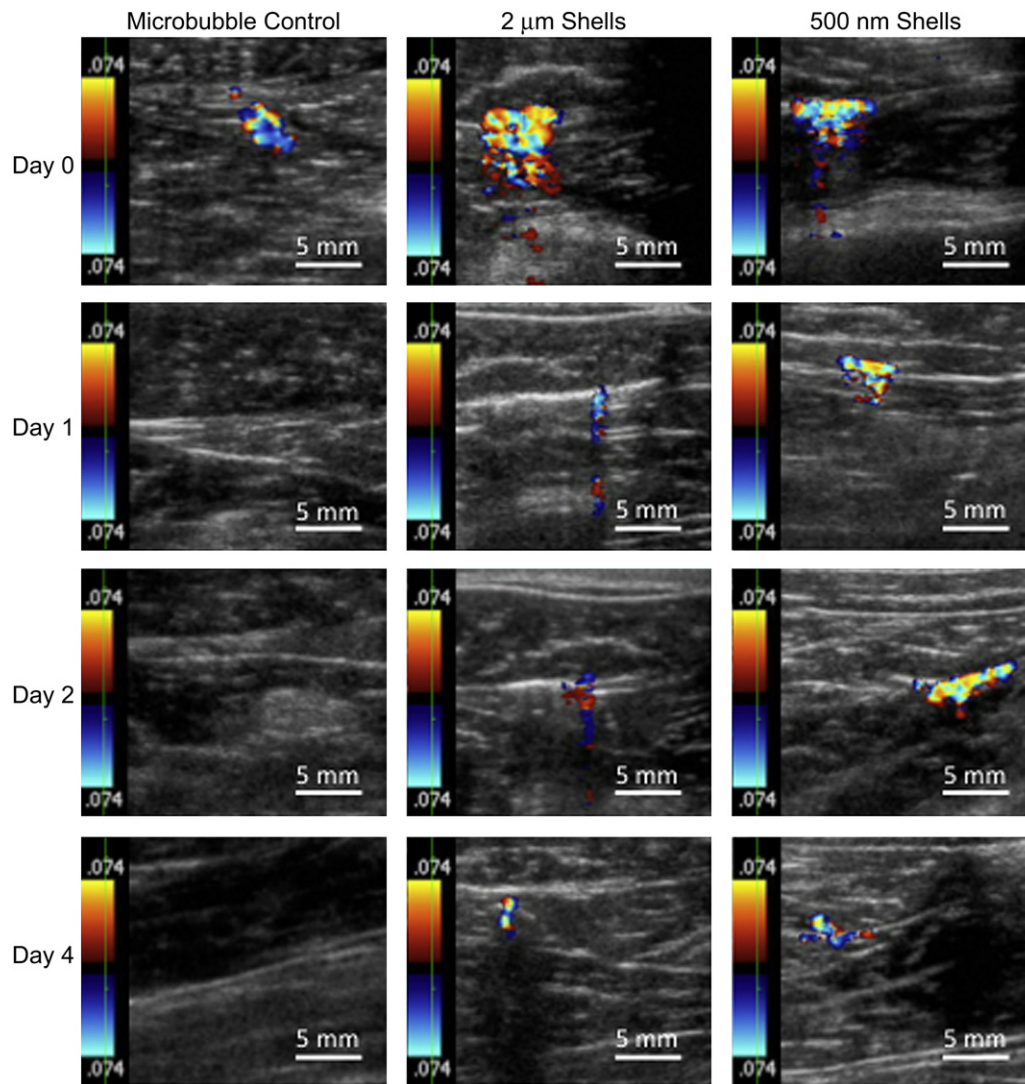


Fig. 6. Persistence in an *in vivo* model. 50 μ l of control microbubbles, 2 μ m shells and 500 nm shells were injected into New Zealand White Rabbit thighs and imaged over the course of four days. Shown in the left columns are the control microbubbles; 50 μ l were injected containing 10^8 microbubbles/ml. All injections were imaged at an MI of 1.9 at 7 MHz with color Doppler using the Siemens Sequoia. Day 0 corresponds to imaging within 15 min of the injection. Note that signal persisted for 4 days when either formulation of silica particles were injected. Microbubbles given as 10^8 (left column) or 10^{10} (not shown) could not be detected 1 day after injection.

4. Discussion

It has been shown *in vitro* that 2 μ m diameter gas filled silica-boron microshells have a maximum continuous imaging time of 48 min and an *in vitro* lifetime up to 5 days. It has been

demonstrated that the 2 μ m gas filled particles exhibit a frequency dependent behavior in which lower clinical US frequencies are favorable for detection, but at 7 MHz, which is applicable for breast imaging, an adequate signal can be achieved at very low particle concentration. The variation in signal with varying MI is consistent

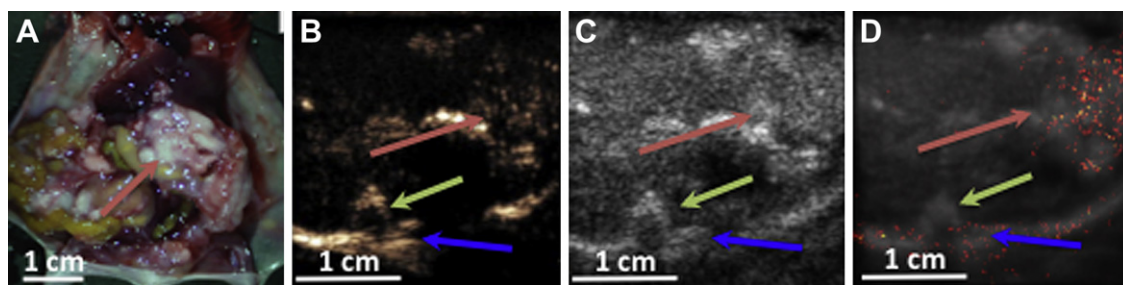


Fig. 7. Testing of gas filled silica microshells in a Mouse. (A) Dissected nu/nu mouse with an interperitoneal IGROV-1 ovarian tumor (red arrow white mass on right side of image). 200 μ g of 2 μ m silica shells diluted into 3 ml of saline and injected into the peritoneum and then perfused into the blood. (B) CPS imaging of the particles through a cross section of the tumor 1 h after quasi IV injection. (C) B-mode image through a cross section of the tumor 1 h after quasi IV injection. (D) Overlay image using several frames from CPS imaging and B-mode to show an integrated heat map of signal from the particles. For all the images, the red arrow points to the tumor, the green arrow points to the spinal column and the blue arrow points to the bottom of the mouse. (For interpretation of the references to colour in this figure legend, the reader is referred to the web version of this article.)

with the existence of subpopulations of particles with varying mechanical strength. *In vitro* lifetime data has been corroborated with an *in vivo* experiment in rabbit thighs demonstrating that the signal generated by the microshells remains detectable for several days. Finally, we showed the feasibility of imaging tumors *in vivo* when a 200 μg dose of 2 μm shells was given intraperitoneally to IGROV-1 tumor bearing mice.

After the 500 nm or 2 μm particle signal was diminished with continuous US imaging, more signal could be generated by increasing the MI. This behavior is consistent with the existence of subpopulations within each given sample that have slightly variable mechanical strengths. This phenomenon may be greatly advantageous in extending the operating imaging time. It is possible to image particles for a period of time at low MI and as the signal diminishes, the MI can be raised slightly further extending the amount of time usable signal is present.

5. Conclusions

For marking and resecting tumors, the duration of continuous US imaging must be long enough to allow the surgeons ample time to reorient themselves for accurate resection. The long *in vitro* and *in vivo* lifetime of gas filled silica nano and microparticles allows the particles to be injected over 24 h before the surgery, allowing greater flexibility for surgical logistics and a heightened level of patient comfort avoiding the use of painful guide wires. Furthermore, *in vivo* tests showed that the particles stay stationary in the injection site even with constant use of a high strain muscle, indicating that these particles can be used as stationary guidance markers. The tests performed using clinical transducers with two different commercial US systems established that these particles can be integrated with existing technologies.

Acknowledgments

This study utilized the Small Animal Imaging Resource supported by the *In vivo* Cancer and Molecular Imaging Center (ICMIC) P50-CA128346. AL is supported by an R25 CA153915 training grant as well as R01CA095298 from the National Cancer Institute. The content is solely the responsibility of the authors and does not necessarily represent the official views of the National Cancer Institute or the National Institutes of Health. ZW is supported by a Career Development Award through the ICMIC. SB is supported by a NIH-IMAT CA151140-01A2 grant. The authors wish to thank Siemens Medical Solutions USA, Inc. for providing the Sequoia US system and Phillips for providing the iU22 as equipment loans to UCSD. The authors would also like to thank Dr. Dwayne Stupack for providing the IGROV-1 tumor bearing mice.

Appendix A. Supplementary data

Supplementary data related to this article can be found online at doi:10.1016/j.biomaterials.2012.03.066.

References

- [1] Klimberg VS, Harms S, Korourian S. Assessing margin status. *Surg Oncol* 1999;(2):77–84.
- [2] Mullenix PS, Cuadrado DG, Steele SR, Martin MJ, See CS, Beitler AL, et al. Secondary operations are frequently required to complete the surgical phase of therapy in the era of breast conservation and sentinel lymph node biopsy. *Am J Surg* 2004;187(5):643–6.
- [3] Singletary SE. Surgical margins in patients with early-stage breast cancer treated with breast conservation therapy. *Am J Surg* 2002;184(5):383–93.
- [4] Gray RJ, Salud C, Nguyen K, Dauway E, Friedland J, Berman C, et al. Randomized prospective evaluation of a novel technique for biopsy or lumpectomy of nonpalpable breast lesions: radioactive seed versus wire localization. *Ann Surg Oncol* 2011;8(9):711–5.
- [5] Gray RJ, Pockaj BA, Karstaed PJ, C.Roarke M. Radioactive seed localization of nonpalpable breast lesions is better than wire localization. *Am J Surg* 2004;188(4):377–80.
- [6] Blair SL, Thompson K, Rococco J, Malcarne V, Beitsch PD, Ollila DW. Attaining negative margins in breast-conservation operations: is there a consensus among breast surgeons? *J Am Coll Surg* 2009;209(5):608–13.
- [7] Nelson HD, Tyne K, Naik A, Bougatsos C, Chan BK, Humphrey L. Screening for breast cancer: an update for the U.S. preventive services task force. *Ann Intern Med* 2009;151(10):727–37. W237–42.
- [8] Turnbull L, Brown S, Harvey I, Olivier C, Drew P, Napp V, et al. Comparative effectiveness of MRI in breast cancer (COMICE) trial: a randomised controlled trial. *Lancet* 2010;375(9714):563–71.
- [9] Berg WA, Blume JD, Cormack JB, Mendelson EB, Lehrer D, Bohm-Velez M, et al. Combined screening with ultrasound and mammography vs mammography alone in women at elevated risk of breast cancer. *J Am Med Assoc* 2008;299(18):2151–63.
- [10] Corsetti V, Houssami N, Ferrari A, Ghirardi M, Bellarosa S, Angelini O, et al. Breast screening with ultrasound in women with mammography-negative dense breasts: evidence on incremental cancer detection and false positives, and associated cost. *Eur J Cancer* 2008;44(4):539–44.
- [11] Ricci P, Cantisani V, Ballesio L, Pagliara E, Sallusti E, Drudi FM, et al. Benign and malignant breast lesions: efficacy of real time contrast-enhanced ultrasound vs. magnetic resonance imaging. *Ultraschall Med* 2007;28(1):57–62.
- [12] Sorelli PG, Cosgrove DO, Svensson WE, Zaman N, Satchithananda K, Barrett NK, et al. Can contrast-enhanced sonography distinguish benign from malignant breast masses? *J Clin Ultrasound* 2010;38(4):177–81.
- [13] Voight JU. Ultrasound molecular imaging. *Methods* 2009;48(2):92–7.
- [14] Sonne C, Xie F, Lof J, Oberdorfer J, Phillips P, Carr Everbach E, et al. Differences in definity and optison microbubble destruction rates at a similar mechanical index with different real-time perfusion systems. *J Am Soc Echocardiogr* 2003;16(11):1178–85.
- [15] De Jong N, Bouakaz A, Frinking P. Basic acoustic properties of microbubbles. *Echocardiogr J Card* 2002;19(3):229–40.
- [16] Tiemann K, Pohl C, Schlosser T, Goenechea J, Bruce M, Veltmann C, et al. Stimulated acoustic emission: pseudo-doppler shifts seen during the destruction of nonmoving microbubbles. *Ultrasound Med Biol* 2000;26(7):1161–7.
- [17] Martinez HP, Kono Y, Blair SL, Sandoval S, Wang-Rodriguez J, Mattrey RF, et al. Hard shell gas-filled contrast enhancement particles for colour doppler ultrasound imaging of tumors. *Medchemcomm* 2010;1(4):266–70.
- [18] Yang J, Sandoval S, Alfaro JG, Aschemeyer S, Liberman A, Martin DT, et al. Red-luminescent europium (III) doped silica nanoshells: synthesis, characterization, and their interaction with HeLa cells. *J Biomed Opt* 2011;6(16):066012.
- [19] Yang J, Lind JU, Troglor WC. Synthesis of hollow silica and titania nanospheres. *Chem Mater* 2008;20(9):2875–7.
- [20] Urban-Klein B, Werth S, Abuharbid S, Czubyko F, Aigner A. RNAi-mediated gene-targeting through systemic application of polyethylenimine (PEI)-complexed siRNA in vivo. *Gene Ther* 2004;12(5):461–6.
- [21] Lu J, Liang M, Li Z, Zink JL, Tamanoi F. Biocompatibility, biodistribution, and drug-delivery efficiency of mesoporous silica nanoparticles for cancer therapy in animals. *Small* 2010;6(16):1794–805.
- [22] Shahani K, Swaminathan SK, Freeman D, Blum A, Ma L, Panyam J. Injectable sustained release microparticles of curcumin: a new concept for cancer chemoprevention. *Cancer Res* 2010;70(11):4443–52.